Electrochemical and Spectroscopic Studies on Triarylamine-Polychlorotriphenylmethyl Dyads with Particularly Strong Triarylamine Donors

Stefanie Breimaier[a] and Rainer F. Winter*[a]

We present two new donor-acceptor dyads composed of a polychlorotriphenylmethyl radical (**PTM•**) as the acceptor (A) and bis(4-dimethylaminophenyl)(phenyl)amine (**TPAN**) or 2,2′:6′,2″:6″,6-trioxytriphenylamine (**TOTA**) as particularly electron-rich triarylamine (**TAA**) donors (D). We assessed their electrochemical properties and electronic structures by cyclic voltammetry, UV/vis/NIR spectroscopy, EPR spectroscopy and quantum chemical calculations. By establishing the spectroscopic fingerprints of the oxidized and reduced forms, we probe for the possible coexistence of a zwitterionic **TAA$^+$-PTM$^-$** valence tautomer (VT), besides neutral **TAA-PTM•**. UV/vis/NIR and EPR spectroscopic studies at variable temperature and in various solvents however provide no indication for such equilibria. Quantitative spin counting experiments by EPR spectroscopy and quantum chemical calculations indicate that the one-electron oxidized forms of these dyads possess an open-shell singlet ground state which is energetically slightly below the triplet state

Introduction

Valence tautomers (VTs) are different electronic isomers of a compound composed of a donor and an acceptor unit. They differ by the redox states adopted by the donor (D or D^+) and the acceptor (A or A^-) and hence by the charge and spin density distributions within the molecule. As individual VTs interconvert via an intramolecular electron transfer (IET) process,[1] the occurrence of valence tautomerism requires that the intrinsic redox potentials of the D/D^+ and the A/A^- redox couples are not too dissimilar. The phenomenon of valence tautomerism was initially observed for transition metal complexes with redox-active, "non-innocent" ligands, particularly those of the *ortho*-benzoquinone/semiquinonate/catecholate type and their many isoelectronic imine or thio variations,[2,3,4] but was later expanded to mixed-valent compounds with chemically inequivalent redox sites.[5,6] Examples of electronic isomers with even more subtle distinctions between two different electronic minima have also appeared in the literature.[7] The fact that isomerization is triggered by external stimuli, such as light irradiation or temperature or pressure changes[8] and that VTs exhibit individually different electronic and spectroscopic properties render them stimuli-responsive building blocks for bistable molecule-based materials like molecular switches and memories.[2,4,6,9]

Some time ago, *Veciana* and co-workers introduced particularly intriguing metal-organic valence tautomeric pairs based on ferrocenyl-perchlorotriphenylmethyl radical dyads **Fc-PTM·** (Figure 1).[10,11,12,13] These dyads exhibited a characteristic, low-energy electronic transition for IET between the Fc donor and the PTM· acceptor in the near infrared (NIR) region of the electronic spectrum. The strong positive solvatochromism (λ_{max} = 892 nm/112190 cm^{-1} in *n*-hexane; 1003 nm/9970 cm^{-1} in DMSO) of this band agrees with a less polar, neutral ground state **Fc-PTM•**.[10] While solution spectra contain only the characteristic absorption bands of the neutral PTM• radical, but none of the PTM^- anion,[10,11,14] Mößbauer spectroscopy on solid samples clearly indicated that the zwitterionic **Fc$^+$-PTM$^-$** state is thermally populated.[11,13,15] When the electron-richness of the Fc donor was increased by introducing eight or nine methyl groups to the Cp ligands, the zwitterionic form was also observed in polar solvents like acetone or dimethylformamide (DMF).[16] Such coexistence of neutral and zwitterionic species in solution was also reported for purely organic **PTM•**-based D–A dyads featuring a tetrathiafulvalene (TTF) instead of a Fc donor and a TTF-oxophenalenoxyl radical dyad.[17,18,19]

[a] *S. Breimaier, Prof. R. F. Winter*
Department of Chemistry
University of Konstanz
Universitätsstraße 10, 78457 Konstanz, Germany
E-mail: stefanie.breimaier@uni-konstanz.de
rainer.winter@uni-konstanz.de

Supporting information for this article is available on the WWW under https://doi.org/10.1002/ejoc.202100476

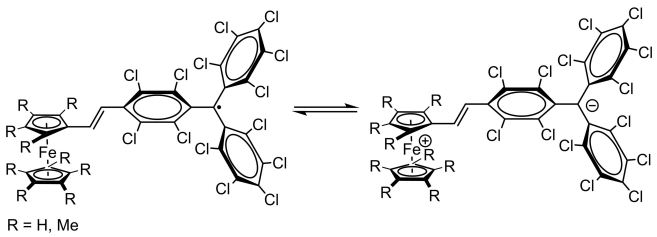

Figure 1. Equilibria between the neutral **Fc-PTM•** and the zwitterionic **Fc$^+$-PTM$^-$** states.

Other examples of purely organic donor-acceptor dyads potentially capable of exhibiting valence tautomerism are triarylamine-PTM• dyads **TAA-PTM•**. The latter constitute rare examples of neutral, purely organic, redox-asymmetric mixed-valence (MV) compounds with a low-energy electronic transition to the **TAA$^+$-PTM$^-$** forms. Several such derivatives as well as a diarylamine-appended PTM• radical were scrutinized for solvent effects on intramolecular charge transfer, taking advantage of the good solubilities in nonpolar solvents and the lack of ion pairing effects.[20–23,24] These studies disclosed, that the degree of electronic coupling between the two dissimilar redox sites is weaker than in mixed-valent bis(triarylamines) with similar π-conjugated linkers. This is due to an inherent redox asymmetry as reflected by the different redox potentials of the donor and the acceptor and the concomitant localization of the β-HOSO on the TAA and the β-LUSO on the PTM• entity, where HOSO and LUSO denote the energetically highest occupied/energetically lowest unoccupied spin orbital.[20–23] Similar work was also performed on various *N*-carbazole-polychlorotriphenylmethyl radicals with a lesser degree of chlorination and hence lower acceptor strengths.[25–30] One representative of these compounds has provided hints as to the presence of small quantities of a zwitterionic valence tautomer in highly polar DMF.[29]

One important setscrew that governs the occurrence and positioning of the valence tautomeric equilibrium is the intrinsic difference between the half-wave potentials for donor oxidation and reduction of the acceptor in such dyads. For all previously studied **TAA-PTM•** dyads, this potential separation $\Delta E_{1/2}$ is larger than 900 mV (> 86 kJ/mol, 5.4 eV). At the other end of the scale, ferrocene-PTM• dyads with the particularly electron-rich octa- and nonamethylferrocene donors exhibit $\Delta E_{1/2}$ values as low as 169 mV. It is these cases, where zwitterionic valence tautomers could be observed in fluid solution.[6,16] Other work has described valence tautomerism in conceptually related ferrocene-diarylmethylium dyads with intrinsic half-wave potential differences as large as 500 mV, albeit in these cases subsequent dimerization of the ferrocenium-trityl isomers, which provides an additional driving force, is entangled with the valence tautomeric equilibria.[31] We therefore mused that **TAA-PTM•** dyads might also be capable of exhibiting valence tautomerism, if particularly strong TAA donors are used. By screening the literature we identified the planar 2,2′:6′,2″:6″,6-trioxytriphenylamine (**TOTA**)[32–34] and bis(4-dimethylaminophenyl)(phenyl) amine as particular promising candidates (see Figure 2). Herein, we present the synthesis as well as the electrochemical, spectroscopic, and electronic properties of the corresponding **TAA-PTM•** dyads and their oxidized and reduced forms as well as the results of solvent- and temperature-dependent UV/vis/NIR and EPR studies as probes of possible valence tautomerism.

Results and Discussion

Synthesis. The required PTM precursors **PTM-PPh$_3$Br** and **PTM-PO(OEt)$_2$** were prepared according to established literature procedures[35] (Scheme 1) via the so-called BMC chlorination

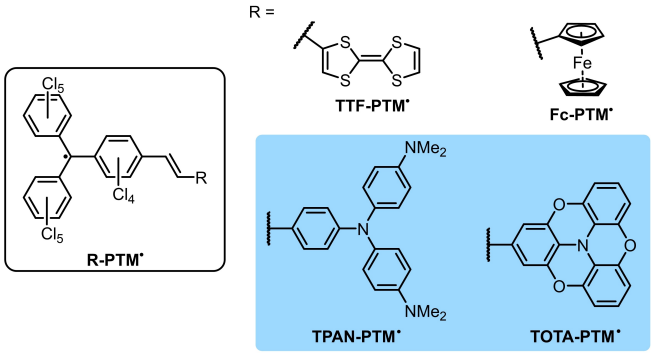

Figure 2. Illustration of the literature-known **TTF-** and **Fc-PTM•** dyads (top) and the new **TAA-PTM•** dyads of the present study (bottom).

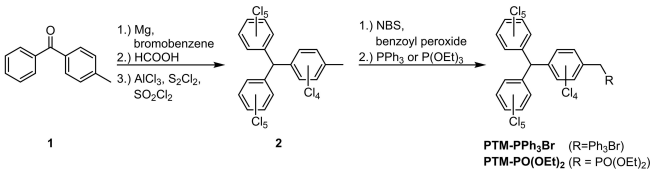

Scheme 1. Synthesis of PTM precursor **PTM-PPh$_3$Br** and **PTM-PO(OEt)$_2$**.

method of Ballester and co-workers.[36] **TOTA** was synthesized according to the literature-known four-step sequence outlined in Scheme 2.[34,37] It was then subjected to a Vilsmeier reaction, which introduced the formyl group. Wittig reaction of **TOTA-CHO**[38] with **PTM-PO(OEt)$_2$** afforded the corresponding triarylmethane derivative **TOTA-PTMH** (Scheme 2) in modest yield.

The synthesis of the second target compound **TPAN-PTM•** is illustrated in Scheme 3. First, the phosphonium salt **PTM-PPh$_3$Br** was reacted with 4-iodobenzaldehyde **7**. The obtained Wittig product **8**[35] was then subjected to a Pd-catalyzed Buchwald-Hartwig amination with bis(4-dimethylaminophenyl)amine to

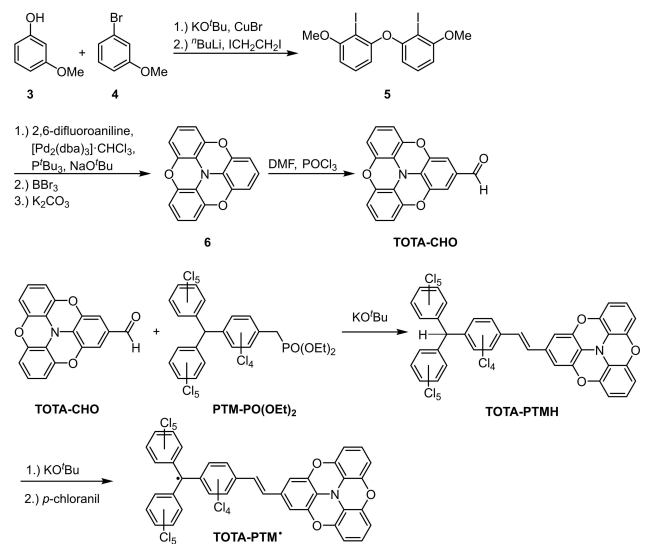

Scheme 2. Synthesis of **TOTA-PTM•**.

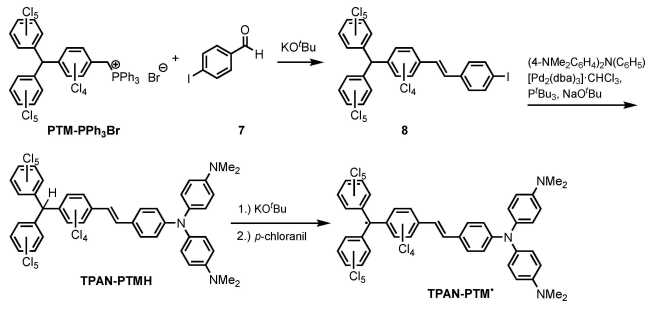

Scheme 3. Synthesis of **TPAN-PTM•**.

afford **TPAN-PTMH**. Both TAA-substituted triphenylamines provided well-resolved ^{1}H and ^{13}C NMR spectra which attest to their spectroscopic purities (see Figures S1 to S4 of the Supporting Information). The target radical dyads were then prepared via the usual two-step sequence involving deprotonation of the triarylmethyl constituent with potassium *tert*-butoxide and subsequent oxidation of the ensuing anions with *p*-chloranil (Scheme 2, Scheme 3).

Electrochemistry. The redox properties of **TOTA-PTM•** and **TPAN-PTM•** were probed by cyclic voltammetry in 0.1 M NBu_4PF_6/CH_2Cl_2 and NBu_4PF_6/DMF at r.t. Representative voltammograms (CVs) in CH_2Cl_2 are shown in Figure 3 and in Figures S7 and S8 of the SI, while the associated data are collected in Table 1. Both radicals exhibit a one-electron wave for the reduction of the PTM• radical to the corresponding carbanion. Increasing the donor strength of the TAA from **TOTA** to **TPAN** shifts the half-wave potential $E_{1/2}^{\bullet/-}$ of this process only slightly cathodic, from −708 mV to = −729 mV. This agrees with

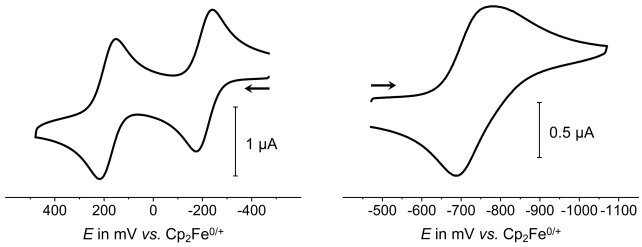

Figure 3. Cyclic voltammograms of the oxidation (left) and reduction (right) of **TPAN-PTM•** in CH_2Cl_2/NBu_4PF_6 (0.1 M) at room temperature and $\nu = 0.1$ Vs^{-1}.

previous findings of Lambert on other TAA-PTM• donor-acceptor dyads.[19] Owing to the presence of very electron-rich TAA donors, the CVs of both dyads also show two consecutive one-electron oxidation waves. Reverse-to-forward peak current ratios *r* of near unity attest to the high degree of chemical reversibility. This also seems to hold for the second oxidation of the TOTA dyad, where the proximity of this wave to the anodic discharge limit prevents us from obtaining meaningful values of *r*. The half-wave potential of the first oxidation of the TOTA derivative of 119 mV is already by ca. 120 mV lower than that of Lambert's most electron-rich di(4-anisyl)(phenyl)amine TAA-PTM• derivative. **TPAN-PTM•** oxidizes at an even lower potential of −205 mV vs. the ferrocene/ferrocenium standard, which brings $\Delta E_{1/2}$ down to 524 mV (Table 1). Changing the solvent to more polar DMF causes a sizable anodic shift of the half-wave potential for PTM• reduction by 300 mV, while causing only smaller (**TPAN-PTM•**) or negligible effects (**TOTA-PTM•**) on those for triarylamine oxidation. This reduces the energy differences between the neutral and the zwitterionic forms considerably.

The origin of the second oxidation wave in these dyads cannot be assigned unambiguously on the basis of CV data alone. While no second oxidations seem to have been reported for **TOTA** and **TPAN**, similar, electron rich triaryl- or *N*,*N*-diaryl-*N*-methylamines were found to undergo further oxidation at ca. 300–400 mV more positive $E_{1/2}$ as the first oxidation and to yield robust, quinoid dications.[39] Similar triarylmethyl-based oxidations were also observed for carbazole-triarylmethyl dyads with only partially chlorinated aryl substituents.[25–30] Lambert and coworkers did nevertheless not observe the oxidation of the PTM• radical entity within their TAA-PTM• dyads up to potentials of 1000 mV.[20,22] On the other hand, the 4-formylstyryl-appended PTM• radical ($C_6Cl_5)_2C$(2,3,5,6-C_6Cl_4–CH=CH–C_6H_4-4-CHO) (**HOC-Sty-PTM•**) was found to oxidize at ca. 590 mV.[40] As we will discuss later, this issue can however be resolved by the spectroscopic characterization of the doubly oxidized forms.

Comparison of the redox potentials for the first oxidation and reduction with those of Veciana's PTM radical **HOC-Sty-PTM•** on the one hand and those of pristine **TOTA** and **TPANH** on the other provides us with a glimpse of how the TAA donor and the PTM acceptor affect each other. Thus, on replacing the formyl acceptor by the $(4\text{-}Me_2NC_6H_4)_2N(C_6H_4)$ donor, $E_{1/2}^{\bullet/-}$ shifts cathodically by a rather moderate margin of ca. 80 mV. For the TOTA-derived dyad this shift is even down to 60 mV.[40] Quite

Table 1. Cyclic voltammetry data of **TOTA-PTM•**, **TPAN-PTM•** and reference compounds.[a]

	$E_{1/2}^{0/+}(\Delta E_p)$ CH_2Cl_2	DMF	$E_{1/2}^{+/2+}(\Delta E_p)$ CH_2Cl_2	DMF	$E_{1/2}^{0/-}(\Delta E_p)$ CH_2Cl_2	DMF	$\Delta E_{1/2}^{0/+//0\cdot}$ CH_2Cl_2	DMF
TOTA-PTM•	119 (65)	124 (59)	932 (86)	–	−708 (115)	−391 (60)	827	515
TPAN-PTM•	−205 (66)	−119 (79)	187 (66)	106 (59)	−729 (94)	−426 (60)	524	307
OHC-Sty-PTM• [b]	590 (–)	–	–	–	−650(–)	–	–	–
TOTA-Br[c]	215 (91)	–	–	–	–	–	–	–
TOTA[d]	110 (–)	–	–	-	–	–	–	–
TPANH[e]	−60 (–)	–	–	–	–	-	–	–

[a] All data in millivolts versus $Cp_2Fe^{0/+}$ in CH_2Cl_2/NBu_4PF_6 (0.1 M) at r.t. and at $\nu = 0.1$ Vs^{-1}. [b] From ref. [40]. [c] See Figure 8 in the Supporting Information. [d] From ref. [33]. [e] From ref. [41].

surprisingly, attaching the nominal –CH=CH-PTM• acceptor to the **TOTA** or the **TPAN**[32,41] donors introduces only a slight anodic shift of 9 mV or even a cathodic shift of 145 mV with respect to their unsubstituted parents. Obviously, the effect of enlarging the π-conjugated system tends to override the inductive influence of the remote acceptor. Both these findings indicate that the TAA donor and the PTM• acceptor are largely decoupled from each other in the electronic ground states of these dyads, which is a necessary prerequisite for observing valence tautomerism.

UV/vis/NIR spectroscopy of the neutral, the reduced and the oxidized forms of the dyads. TOTA-PTM• and **TPAN-PTM•** are red-colored in the solid state and in solution and exhibit an intense, structured absorption band with two distinct peaks at 389 nm and at 408 nm or 414 nm, respectively, in CH_2Cl_2 (Figure 4, Table 2). The 389 nm band is the characteristic fingerprint of the PTM• radical and was observed at an identical wavelength in several other oligophenylenevinylene- (OPV-) appended mono- or OPV-bridged bis(PTM•) diradicals[40] and in other previously reported donor-PTM dyads.[10,18,42,43,44]

The results of time-dependent (TD)-DFT calculations at the pbe1-pbe-DFT level of theory also agree with this assignment. Comparisons between experimental and computed spectra, the compositions of the relevant MOs and the corresponding electron density difference maps (EDDMs) can be found as Figures S9 to S13 and Tables S1 and S2 in the Supporting Information. According to these calculations, all other electronic bands at lower excitation energies involve, to various degrees, charge transfer (CT) from the TAA donor to the PTM• acceptor, similar to what has been reported for other OPV- and donor-appended PTM• radicals.[10,40,42,44] This is particularly true for the most red-shifted absorption band, which is adequately described as the β-HOSO→β-LUSO transition and hence corresponds to an intramolecular electron transfer.[10,13,18,42,45] In agreement with the ca. 300 mV lower half-wave potential difference $\Delta E_{1/2}$ between TAA oxidation and PTM• reduction, the underlying transition is red-shifted from 819 nm for the TOTA- to 973 nm for the TPAN-derivative and its intensity is increased by a factor of 2. In further support of its CT character, this band also proved to be solvatochromic (Figure 4 and Figure S30 in the Supporting Information).

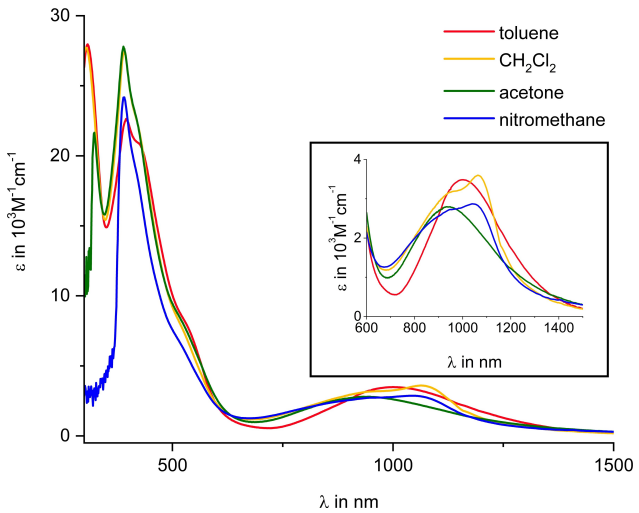

Figure 4. UV/vis/NIR spectrum of **TPAN-PTM•** in toluene (red), CH_2Cl_2 (orange), acetone (green) and nitromethane (blue).

Table 2. UV/vis/NIR spectroscopic data for **TOTA-PTM^{n+}** and **TPAN-PTM^{n+}** in their neutral, anionic, monocationic and dicationic states.[a]

	n	λ_{max} (ε[10^3 M^{-1} cm^{-1}])
TOTA-PTM•	0	389 (24.7). 408 (20.6), 532 (3.4), 819 (1.6)
	−1	412 (13.5), 517 (18.9), 581 (18.6)
	+1	389 (24.8), 475 (15.6), 671 (10.4), 716 (17.1), 793 (3.6), 968 (2.9)
TPAN-PTM•	0	389 (27.4), 414 (22.4), 512 (7.7), 973 (3.2)
	−1	397 (16.7), 527 (18.5), 562 (18.0)
	+1	389 (27.5). 412 (23.2), 506 (8.9), 729 (7.3), 1082 (27.5)
	+2	386 (20.0), 420 (14.4), 630 (14.8), 786 (40.3)

[a] Data are reported in nm. Measurements were carried out in 1,2-$C_2H_4Cl_2$/NBu_4PF_6 at room temperature.

In order to obtain additional insights into the electronic characteristics of the corresponding oxidized and reduced forms of these dyads, which mirror the individual TAA^+ or PTM^- sites of the CT excited state or of a possible zwitterionic TAA^+-PTM^- valence tautomer, we monitored the concomitant changes of the UV/vis/NIR spectra by in situ electrolysis in a spectroelectrochemical (SEC) setup, employing an optically transparent thin-layer electrolysis (OTTLE) cell.[46] Figure 5 provides graphical accounts of the spectral changes on reduction as well as on the first and on the second oxidation. Experimental data are collected in Table 2. All redox processes except for the second oxidation of the **TOTA-PTM•** dyad proceeded smoothly with clear isosbestic points. For **TOTA-PTM•**, the required high voltages prevented full conversion to the dioxidized form and induced partial decomposition on continued electrolysis. Otherwise, the original spectra of the neutral compounds were fully recovered on reoxidation of the **TAA-PTM$^-$** anions or rereduction of the oxidized forms.

Reduction of the present **TAA-PTM•** dyads induces similar spectroscopic changes as those observed for the previous congeners.[22] Thus, the intensity of the PTM• absorption at 389 nm decreases with a concomitant shift of the remaining absorption to lower energies, while the CT band in the NIR vanishes (see left panel of Figure 5). At the same time, two likewise intense bands at ca. 520 nm and at 562 nm or 581 nm grow in. According to our TD-DFT calculations, these transitions involve CT from mainly the reduced methanide center to either the electron poor C_6Cl_5 entities or the C_6Cl_4-CH=CH linker (see Figures S14 to S18 and Tables S3 and S4 of the Supporting Information) with some admixture of CT from the TAA-based donor to the linker-based LUMO + 1.

The first oxidation the dyads induces even more significant changes of the electronic spectra. We first note a slight intensification of the characteristic PTM• absorption band. Secondly, the originally poorly resolved CT transitions at ca. 510–530 nm shift slightly hypsochromically and evolve into clear bands. The most remarkable alterations are the appearance of two new low-energy absorption bands. The most prominent of these is a vibrationally structured, intense band

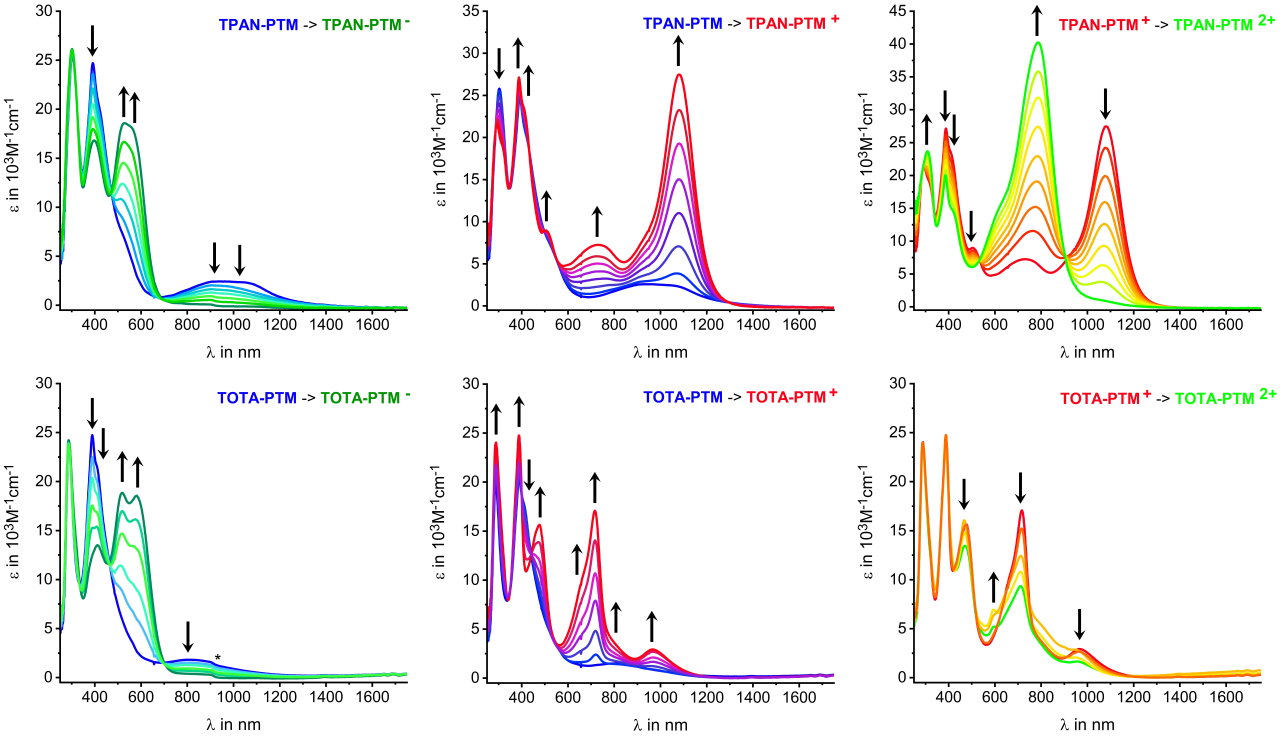

Figure 5. UV/vis/NIR spectroelectrochemistry of **TPAN-PTM•** (top panels) and **TOTA-PTM•** (bottom panels) during the reduction (left) as well as the first (middle) and the second oxidation (right) in an OTTLE cell (1,2-$C_2H_4Cl_2$/NBu_4PF_6 (0.1 M), at r.t.). The asterisk marks an artefact caused by our instrumentation.

peaking at 716 nm or 1082 nm, which corresponds to the oxidized TAA donor.[47] We also note a close resemblance of the low-energy band of the **TOTA**$^+$ chromophore to that reported for other salts of this cation.[32,48] The second feature is a less intense, unstructured band which is either disposed to lower (**TOTA**$^+$**-PTM•**) or higher (**TPAN**$^+$**-PTM•**) energies compared to the TAA$^+$ band.

Accompanying (TD)-DFT calculations place the triplet state 52 kJ/mol (**TOTA**$^+$**-PTM•**) or 44 kJ/mol (**TPAN**$^+$**-PTM•**) below the closed-shell singlet state, but slightly above the open-shell singlet (see below). We also note that the TD-DFT computed spectra of the diradical forms show an overall better agreement with the experimental spectra than those computed for the closed-shell singlet states (see Figures S19 and S20 and Tables S5 to S8 of the Supporting Information), for which only one or two transitions with relevant oscillator strengths are predicted. The results of our TD-DFT analysis confirm the assignment of the most intense, low-energy band as a ππ* transition within the oxidized TAA$^+$ chromophore subunit, augmented with some CT from the PTM• moiety for **TOTA**$^+$**-PTM•**. The broad band of **TPAN**$^+$**-PTM•** at 729 nm is caused by a β-HOSO-1→β-LUSO transition and represents CT from the –C_6Cl_4-CH=CH > C- > linker to the **TPAN**$^+$ moiety, in agreement with other oxidized TAA-PTM• derivatives.[22,23] The 968 nm band of **TOTA**$^+$**-PTM•** is likely of similar origin although our computations failed to produce such a transition.

As was already mentioned, we could only achieve partial conversion of **TOTA**$^+$**-PTM•** to the corresponding dication before the onset of decomposition, which is indicated by the gradual loss of the initial isosbestic points and the lack of reversibility on back electrolysis. No such problems were encountered for **TPAN-PTM•**. During the second oxidation, the prominent band at 1082 nm vanishes and is replaced by an even more intense absorption with a similar vibrational structuring at 786 nm. According to our TD-DFT calculations, this band originates from two close-lying transitions, which correspond to CT from the styryl-PTM• moiety to the doubly oxidized N(C_6H_4-4-NMe_2) group and a ππ* transition confined to the oxidized TAA^{2+} chromophore itself (see Figures S25 and S29 and Tables S9 and S10 of the Supporting Information). This finally confirms the **TPAN** donor of the **TPAN-PTM•** dyad as the relevant electron transfer site of also the second oxidation step.

After having identified the double band at ca. 520 nm and at 560 or 580 nm as the spectroscopic fingerprints of the reduced PTM$^-$ and the transition near 800 nm or 1100 nm to the aminium-centered absorption of the oxidized TAA$^+$ constituents of our dyads, we recorded UV/vis/NIR spectra of the neutral compounds in several solvents of different polarity in order to probe for the possible presence of a second, zwitterionic valence tautomer (see Figure 4 and Figure S30 in the Supporting Information). Electronic spectra of both dyads however provided no conspicuous features that would point to the existence of such a species. One should note here that the band structuring in some solvents is likely due to a vibrational progression, as it was observed on earlier occasions for similar systems.[22] This is also supported by the lack of spectral

changes for the **TPAN-PTM•** dyad on varying the temperature from −70 °C up to 40 °C in CH_2Cl_2 in or *N,N*-dimethylformamide as shown in Figure S31 of the Supporting Information. All things considered, the electronic spectra of the two new **TAA-PTM•** dyads provide no hints to the presence of a second, zwitterionic isomer in solution.

EPR spectroscopy on the parent radicals and their oxidized and reduced forms. Their unpaired spin renders **TOTA-PTM•** and **TPAN-PTM•** EPR active. In the presence of valence tautomerism, one would expect an additional EPR resonance for the second isomer with the unpaired spin density on the aminium instead of the PTM site and with slightly different *g* values and hyperfine splitting (hfs) patterns. EPR spectroscopy of the radicals was initially performed in CH_2Cl_2 and the individual hfs constants were determined by digital simulations (see Figure 6 and Table 3).

The EPR spectrum of **TOTA-PTM•** consists of a doublet resonance with a *g*-value of 1.9949 and coupling constants of $A(^1H) = 2.7$ G, $A(^{13}C) = 13.9$ G (2 C atoms) and $A(^{13}C) = 13.0$ G (4 C atoms), while the EPR signal of **TPAN-PTM•** only reveals as a single resonance line with coupling constants of $A(^{13}C) = 12.0$ G (4 C atoms) and $A(^{13}C) = 13.9$ G (2 C atoms) as derived from the small, additional features on either side of the main peak.[29,49][47] This matches with our DFT calculations, which indicated a PTM• centered spin (see Figure 7). We next recorded *T*-dependent EPR spectra of **TOTA-PTM•** and **TPAN-PTM•** in a solvent of lower (toluene) and higher polarity (DMF) than dichloromethane. No conspicuous changes of the signal could be observed in either toluene or DMF over a temperature range from -60 °C to 100 °C or 120 °C, apart from the expected increase/decrease of the signal intensity upon cooling/warming according to the Boltzmann distributions between the ground and the excited states (see Figures S32 and S33 of the SI).

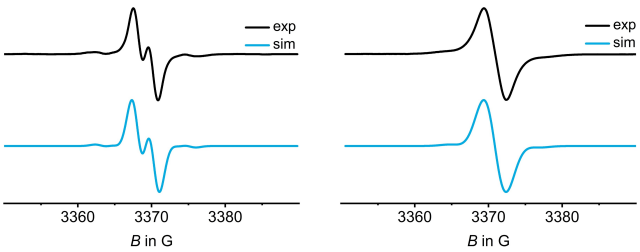

Figure 6. Experimental (black) and simulated (blue) EPR spectra of **TOTA-PTM•** (left) and **TPAN-PTM•** (right) in CH_2Cl_2 at room temperature.

Table 3. EPR data of the target compound **TOTA-PTM•** and **TPAN-PTM•** in their neutral, monocationic and dicationic states.[a]

	g_{iso}	$A(^1H)$	$A(^{13}C)$	$A(^{14}N)$
TOTA-PTM•	1.9949	2.7	13.9 (2 C), 13.0 (4 C)	–
TOTA•⁺-PTM•	1.9936	3.8, 2.4	–	11.1
TPAN-PTM•	1.9945	–	13.9 (2 C), 12.0 (4 C)	–
TPAN•⁺-PTM•	1.9938	–	–	8.2
	1.9938	2.2	–	–
TPAN²⁺-PTM•	1.9942	2.7, 0.7	16.8 (2 C), 13.5 (4 C)	–

[a] All hyperfine coupling constants are reported in Gauss. The monocation of **TPAN-PTM•** was generated with ferrocenium hexafluorophosphate, while the other mono- and dications are generated with acetylferrocenium hexafluoroantimonate as the oxidant.

Samples of the monocations for EPR studies were prepared by chemical oxidation of the neutral compounds, using acetylferrocenium hexafluoroantimonate (**TOTA-PTM•**) or ferrocenium hexafluorophosphate (**TPAN-PTM•**) as the oxidant. The purity of these samples was verified by comparing their UV/vis/NIR spectra to those collected in our spectroelectrochemical measurements. Likewise, dioxidized **TPAN²⁺-PTM•** was prepared by chemical oxidation of the neutral compound with 2.1 equiv. of acetylferrocenium hexafluoroantimonate. The corresponding data are displayed in Figure S34–S36 of the SI. EPR spectroscopy confirms the presence of paramagnetic species by virtue of strong resonance signals. Cation **TOTA⁺-PTM•** does not show separate signal sets for the two different kinds of EPR active subunits, which suggests that their *g* values are basically identical. While broad and ill-resolved at r.t., the signal gradually evolves into a well-defined, non-binomial triplet resonance on cooling with a ^{14}N hyperfine splitting of 11.1 G and additional, partially resolved hyperfine splittings $A(^1H) = 3.8$ G and $A(^1H) = 2.4$ G. Cation **TPAN⁺-PTM•** shows an even poorer resolution, but apparently consists of two different subspectra, one showing a hyperfine splitting $A(^{14}N) = 8.2$ G, and one with a hyperfine splitting $A(^1H) = 2.2$ G, both with a *g* value of 1.9938. These results match with our DFT calculations, which indicate almost uniform spin distributions over the entire molecule with equal spin densities at the TAA•⁺ and the PTM• subunits (see Figure 8). In no case we could observe a half-field signal for the nominally forbidden $\Delta m_s = 2$ transition, which indicates that the coupling constant *J* is small (i.e. the unpaired spins in these diradicaloid species behave essentially independently). This is consistent with the rather large distance of > 12 Å between the nominal spin-bearing centers as derived from the geometry-optimized structures.[50] DFT calculations indicate that the open-

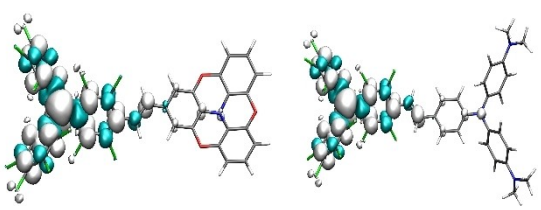

Figure 7. Calculated spin density maps of **TOTA-PTM•** (left) and **TPAN-PTM•** (right).

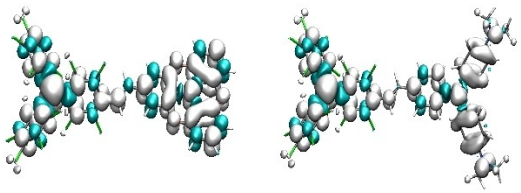

Figure 8. Calculated spin density maps of the monocations **TOTA⁺-PTM•** (left) and **TPAN⁺-PTM•** (right).

shell singlet and triplet states are nearly isoenergetic with a very slight preference (ca. 0.6 kJ/mol) for the former. Quantitative spin counting experiments on **TPAN$^+$-PTM$^•$** with stable DPPH$^•$ as the calibrant indicated, that the open-shell singlet is indeed the ground state and that, at r.t., the triplet state is thermally populated and accounts for ca. 40% of the sample with a further decrease as T is lowered, e.g. to 32% at −50 °C.

The **TPAN^{2+}-PTM$^•$** dication shows a resolved doublet resonance at a g value of 1.9942 and hyperfine coupling constants $A(^1H)$ of 2.7 G and 0.7 G to one proton each, and $A(^{13}C)$ of 16.8 G two and of 13.5 G to four equivalent C atoms. The close resemblance to the spectrum of neutral **TPAN-PTM$^•$** confirms double oxidation at the TAA site. This annihilates the TPAN-based spin, but leaves that of the **PTM$^•$** radical unaltered.

Conclusions

We report on two new donor-acceptor dyads that comprise of a 2,2′:6′,2″:6″,6-trioxytriphenylamine (**TOTA**) or bis(4-dimethylaminophenyl)(phenyl)amine (**TPAN**) donor and a polychlorotriphenylmethyl (PTM$^•$) acceptor unit. Cyclic voltammetry revealed a PTM$^•$-based one-electron reduction and two consecutive TAA-based one-electron oxidations, whose half wave potentials shift cathodically as the electron-releasing capability of the TAA donor increases (**TOTA** < **TPAN**). Half-wave potential differences between the first oxidation and the reduction are notably lowered by ca. 300 mV as the solvent polarity is increased from CH_2Cl_2 to DMF, attesting to a lower energy gap between the neutral **TAA-PTM$^•$** ground state and the excited zwitterionic **TAA$^+$-PTM$^-$** state. The UV/vis/NIR spectra of **TOTA-PTM$^•$** and **TPAN-PTM$^•$** exhibit the characteristic absorption band of the **PTM$^•$** chromophore, as well as a broad, solvatochromic NIR band that can be assigned to an intramolecular electron transfer between the respective TAA donor and the PTM$^•$ acceptor. UV/vis/NIR spectroelectrochemistry confirmed the identity of the individual redox sites and established the spectroscopic fingerprints of the **PTM$^-$** and the **TAA$^{•+}$** chromophores. None of these features was observed in solutions of the neutral dyads. EPR spectra of the native radicals also failed to identify a possible zwitterionic isomer. Quantitative spin counting EPR spectroscopy and DFT calculations indicate that the open-shell singlet and triplet states of the one-electron oxidized forms are nearly degenerate. UV/Vis/NIR and EPR spectroscopy also allow us to safely identify the **TPAN** donor as the site of the second oxidation.

Experimental Section

General procedures. All syntheses were performed under nitrogen atmosphere using standard Schlenk techniques. The solvents for synthesis and characterization were dried over the appropriate drying agent, distilled, stored under nitrogen atmosphere prior to use. All reagents were purchased from commercial suppliers and were used without additional purification. ^1H and ^{13}C NMR spectra were recorded on a Bruker AVANCE III 400 and a Bruker AVANCE III 600 spectrometer at room temperature. The residual signal of the protonated solvents was used as the reference and coupling constants are given in Hertz. Mass spectra were recorded on a LTQ Orbitrap Velos (Thermo Scientific) with ESI capable of a resolution at least 60000. The spectrometer was calibrated with the Pierce LTQ Velos ESI Positive Calibration Solution (Thermo Fisher Scientific) prior to every measurement. Detection was done in the positive-ion mode.

Cyclic voltammetry was performed in a custom-made one-compartment cell with a platinum wire counter electrode and a Ag/AgCl wire pseudoreference electrode. A platinum electrode (ø = 1.1 mm, BASi) was used as working electrode and polished with diamond pastes from Buehler and Wirtz with successively decreasing particle sizes of 1.5 μm and 1 μm prior to the experiment. CH_2Cl_2/NBu_4PF_6 (0.1 M) was used as supporting electrolyte and the cell was connected to an argon gas bottle. The voltammograms were recorded by a computer-controlled BASi EPSILON potentiostat. Referencing was performed by adding appropriate quantities of cobaltocenium hexafluorophosphate (Cp_2Co^+ PF_6^-) as the internal standard after all scans of interest had been carried out. All potentials are reported against ferrocene/ferrocenium ($Cp_2Fe^{0/+}$) reference couple with $E_{1/2}$ (Cp_2Co^+) PF_6^- = −1330 mV vs. $Cp_2Fe^{0/+}$ under our conditions. Redox potentials are subject to an error of ±3 mV.

UV/vis/NIR spectroelectrochemistry was carried out in a custom-built OTTLE cell[46] featuring two CaF_2 windows of a conventional liquid IR cell with a Pt-mesh working and counter electrode and a thin silver foil as reference electrode sandwiched in between. 1,2-$C_2H_4Cl_2/NBu_4PF_6$ (0.1 M) was used as the supporting electrolyte. The UV/vis/NIR measurements were performed on a diode-array TIDAS spectrometer by J&M ANALYTIK AG with a spectroscopic window of 250–2100 nm. The applied voltage was adjusted with the potentiostat Wenking Pos2 from Bank Electronics – Intelligent Controls GmBH.

EPR spectroscopy was performed on a MINISCOPE 400MS X-band benchtop spectrometer by Magnettech GmbH with a temperature controller from the same manufacturer as thermostat. Low-temperature measurements were performed by cooling with liquid nitrogen. For cooling the magnet, a Thermo Fischer Scientific Inc. HAAKE A10 cooling unit was used. The compounds were chemically oxidized with ferrocenium hexafluorophosphate or acetylferrocenium hexafluoroantimonate and dissolved in CH_2Cl_2 at room temperature prior to measuring. Simulations of the experimental EPR spectra were performed using the MATLAB *Easyspin* program.[51] Quantitative spin counting experiments employed the DPPH$^•$ radical standard as the calibrant. Its purity was checked by titration with hydroquinone using a UV/Vis/NIR probe prior to measurements.[52] Further details as to the employed procedures are provided in the Supporting Information. Experimental settings were adjusted as follows to avoid any overmodulation and saturation effects: microwave frequency of 9.4 GHz, microwave attenuation of 36 dB (corresponds to 0.05 mW of microwave power), modulation amplitude of 3 G, sweep width of 6000 G, and a number of 8192 data points.

DFT calculations were carried out using the *Gaussian 16* program package.[53] Geometry optimization was followed by vibrational analysis with the polarizable continuum model (PCM) performed in 1,2-dichloroethane as solvent.[54] Using the TD-DFT method the electronic spectra were calculated at the optimized ground-state structures. Polarized douple-ζ basis sets [6-31G(D), geometry optimization] were employed together with the pbe1pbe functional.[55] In TD-DFT calculations the solvation effects were modelled by the polarizable continuum model.[54] The GaussSum,[56] Avogadro, GNU Parallel, and vmd program packages were used in

combination with POV-Ray[57] for data processing and graphical representations.[57,58]

Synthesis and Characterization.

Diphenyl(p-tolyl)methanol.[59] To a suspension of 3.10 g (127 mmol, 1.25 eq.) of magnesium turnings in 20 mL of dry diethyl ether, 0.43 mL (0.94 g, 5 mmol, 0.05 eq.) of 1,2-dibromoethane were added. 13.33 mL of bromobenzene (20.00 g, 127 mmol, 1.25 eq.), dissolved in 35 mL of dry diethyl ether, were slowly added and the brownish reaction mixture was stirred for further 30 min after addition was complete. 20.00 g (102 mmol, 1.00 eq.) of 4-methylbenzophenone were dissolved in 45 mL of dry diethyl ether and were slowly added. The mixture was stirred for 3 h at 60 °C. After the mixture was cooled in an ice bath, 100 mL of 3 M hydrochloric acid were added, and the organic phase was washed with H_2O (3× 300 mL) and brine (1×300 mL). The organic phase was dried over $MgSO_4$ and the solvent was evaporated. The resulting yellow oil was recrystallized from *n*-hexane to obtain a white solid (yield: 5.18 g, 19%). ^{1}H NMR (400 MHz, $CDCl_3$): δ [ppm] = 7.36–7.28 (m, 10H, H_{phenyl}), 7.18, 7.14 (each d, $^3J_{H\text{-}H}$ = 8.3 Hz, 2H, H_{tolyl}), 2.79 (s, 1H, O*H*), 2.37 (s, 3H, CH_3). ^{13}C NMR (151 MHz, CD_2Cl_2): δ [ppm] = 147.2 (s), 144.1 (s), 137.0 (s), 128.7 (s), 128.0 (s), 128.0 (s), 128.0 (s), 127.3 (s), 82.0 (s), 21.2 (s).

4-Methylbenzophenone ***1***.[59] 4.327 g (15.8 mmol, 1.0 eq.) of diphenyl (*p*-tolyl)methanol were dispersed in 100 mL of 98% formic acid and the mixture was stirred at 99 °C for 3 d. 40 mL of H_2O were added, and the solution was neutralized with K_2CO_3 while being cooled in an ice bath. The phases were separated, and the organic phase was washed with H_2O (3×500 mL) and dried over $MgSO_4$. The solvent was removed to provide a viscous oil (yield: 3.40 g, 83%). ^{1}H NMR (400 MHz, $CDCl_3$): δ [ppm] = 7.37–7.33 (m, 4H, $H_{meta\text{-}phenyl}$), 7.29–7.28 (m, 2H, $H_{para\text{-}phenyl}$), 7.21–7.16 (m, 6H, $H_{ortho\text{-}tolyl}$, $H_{ortho\text{-}phenyl}$), 7.10-7.08 (m, 2H, $H_{meta\text{-}tolyl}$), 5.60 (s, 1H, Ar_3CH), 2.40 (s, 3H, CH_3). ^{13}C NMR (151 MHz, CD_2Cl_2): δ [ppm] = 144.3 (s), 141.1 (s), 135.9 (s), 129.6 (s), 129.5 (s), 129.1 (s), 128.4 (s), 126.4 (s), 56.6 (s), 21.1 (s).

6,6′-((2,3,5,6-Tetrachloro-4-methylphenyl)methylene)bis(1,2,3,4,5-pentachlorobenzene) **2**.[36] 0.68 g (5.1 mmol, 0.38 eq.) of $AlCl_3$ and 0.80 mL (1.36 g, 10.1 mmol, 0.76 eq.) dicholordisulfane were dissolved in 110 mL of sulfuryl chloride. The mixture was heated to 70 °C under protection from light and a solution of 3.25 g (12.6 mmol, 1.00 eq.) of 4-methylbenzophenone (**1**) in 260 mL of sulfuryl chloride was slowly added. Refluxing was continued for 22 h. During that time another 200 mL of sulfuryl chloride were added in portions so as to keep the volume of the reaction mixture constant. The solvent was removed and 15.00 g of $NaHCO_3$ in 500 mL of H_2O were added. The mixture was stirred at 120 °C for 1 h. The solution was acidified with conc. HCl and heated to 120 °C for 1 h. After cooling to r.t. the aqueous phase was removed and the residue was suspended in diethyl ether. The white precipitate was filtered off and washed several times with diethyl ether to give a white powder (yield: 3.50 g, 34%). ^{1}H NMR (400 MHz, $CDCl_3$): δ [ppm] = 6.99 (s, 1H, Ar_3CH), 2.63 (s, 3H, CH_3). ^{13}C NMR (151 MHz, CD_2Cl_2): δ [ppm] = 137.6 (s), 136.8 (s), 136.8 (s), 135.3 (s), 135.1 (s), 134.5 (s), 134.4 (s), 134.1 (s), 134.1 (s), 133.7 (s), 133.7 (s), 133.6 (s), 133.4 (s), 132.6 (s), 132.5 (s), 56.6 (s), 20.8 (s).

6,6′-((4-(Bromomethyl)-2,3,5,6-tetrachlorophenyl)methylene)bis-(1,2,3,4,5-pentachlorobenzene) **PTM-Br**.[60] 2.000 g (2.70 mmol, 1.00 eq.) of compound **2**, 0.445 g (1.47 mmol, 0.54 eq.) of activated benzoyl peroxide and 0.651 g (3.66 mmol, 1.35 eq.) of *N*-bromosuccinimide were dissolved in 60 mL of tetrachloromethane and stirred for 4 d at 85 °C. The suspension was filtered off and the solution was concentrated under vacuum. The solid was washed with *n*-hexane and acetone to obtain the product as a beige solid (yield: 1.83 g, 83%). ^{1}H NMR (400 MHz, $CDCl_3$): δ [ppm] = 7.00 (s, 1H, Ar_3CH), 4.82 (s, 2H, CBrH_2). ^{13}C NMR (151 MHz, CD_2Cl_2): δ [ppm] = 138.1 (s), 136.4 (s), 136.4 (s), 135.2 (s), 135.2 (s), 135.1 (s), 134.8 (s), 134.1 (s), 134.1 (s), 134.1 (s), 133.9 (s), 133.7 (s), 133.7 (s), 132.7 (s), 132.7(s), 56.7 (s), 29.0 (s).

4-[Bis(perchlorophenyl)methyl]-2,3,5,6-tetrachlorobenzyl)-triphenylphos-phonium bromide **PTM-PPh$_3$Br**.[35] 1.00 g (1.22 mmol, 1.00 eq.) of **PTM-Br** and 0.50 g (1.90 mmol, 1.56 eq.) of triphenylphosphine were dissolved in 50 mL of dry benzene and stirred for 20 h at 80 °C. The resulting solid was filtered off and washed with benzene to give the product as a white solid (yield: 1.10 g, 83%). ^{1}H NMR (400 MHz, $CDCl_3$): δ [ppm] = 7.86–7.66 (m, 15H, P(C_6H_5)$_3$), 6.90 (d, $^2J_{H\text{-}H}$ = 1.6 Hz, Ar_3CH), 5.89 (d, 2H, $^2J_{H\text{-}H}$ = 14.4 Hz, CH_2PPh_3Br). ^{13}C NMR (151 MHz, CD_2Cl_2): δ [ppm] = 138.6 (d, $^4J_{CP}$ = 3 Hz, $C_{p,}$ P^+Ph_3), 136.0 (s), 135.3 (s), 134.5 (s), 134.3 (s), 133.8 (s), 133.6 (d, $^2J_{CP}$ = 11 Hz, $C_{o,}$ P^+Ph_3), 132.8 (s), 130.5 d, $^3J_{CP}$ = 13 Hz, $C_{m,}$ P^+Ph_3) (s), 130.3 (s), 128.4 (s), 118.3 (d, J_{CP} = 88 Hz, $C_{ipso,}$ P^+Ph_3), 56.7 (s), 33.0 (d, J_{CP} = 56 Hz, $CH_2P^+Ph_3$).

4-[Bis(perchlorophenyl)methyl]-2,3,5,6-tetrachlorobenzyl-phosphonate **PTM-PO(OEt)$_2$**.[35] 2.000 g (2.44 mmol, 1.00 eq.) of **PTM-Br** and 2.50 mL (2.420 g, 14.57 mmol, 5.97 eq.) of $P(OEt)_3$ were heated to reflux at 155 °C for 130 min. 17 mL of H_2O were added and heating to reflux was continued for further 40 min. After cooling to room temperature, the solution was extracted with $CHCl_3$ (3×40 mL). The combined organic phases were dried over $MgSO_4$ and the solvent was evaporated. Purification was achieved by silica gel column chromatography (*n*-pentane, yield: 0.98 g, 46%). ^{1}H NMR (400 MHz, $CDCl_3$): δ [ppm] = 7.00 (s, 1H, Ar_3CH), 4.09 (q, $^3J_{H\text{-}H}$ = 7.1 Hz, 4H, $POCH_2$), 3.77 (d, $^2J_{H\text{-}P}$ = 22.6 Hz, 2H, $PhCH_2$), 1.27 (t, $^3J_{H\text{-}H}$ = 7.1 Hz, 6H, $POCH_2CH_3$). ^{13}C NMR (151 MHz, CD_2Cl_2): δ [ppm] = 136.6 (s), 135.0 (s), 134.0 (s), 133.8 (s), 133.7 (s), 133.0 (s), 132.9 (s), 132.6 (s), 62.7 (dd, $^2J_{CP}$ = 6.8 Hz, J = 1.7 Hz), 56.7 (s), 16.5 (d, $^3J_{CP}$ = 6.4 Hz).

Bis(3-methoxyphenyl)ether.[37] 11.82 g (0.11 mol, 1.00 eq.) of KO^{t}Bu were suspended in 20 mL of dry DMF and 11.34 mL (12.82 g, 0.10 mol, 0.98 eq.) of 3-methoxyphenol **3** in 10 mL of dry DMF were added slowly. The dark solution was heated to reflux for 1 h and 13.24 mL (19.71 g, 0.11 mol, 1.00 eq.) of 3-bromoanisole, **4**, and 15.12 g (0.11 mol, 1.00 eq.) of CuBr were added. After heating to reflux for 4 h the solvent was removed, and the solid residue was dissolved in diethyl ether. The organic phase was washed with 0.5 M HCl (1×100 mL), 0.5 M NaOH (5×100 mL) and brine (1× 100 mL), dried over Na_2SO_4 and the solvent was removed under vacuum. Purification followed by silica gel column chromatography using *n*-pentane as eluent (yield: 3.73 g, 15%). H NMR (400 MHz, $CDCl_3$): δ [ppm] = 7.26-7.18 (m, 2H, *H*1), 6.70-6.55 (m, 6H, *H*2-4), 3.78 (s, 6H, CH_3). ^{13}C NMR (151 MHz, CD_2Cl_2): δ [ppm] = 161.1 (s), 158.3 (s), 130.2 (s), 111.2 (s), 109.1 (s), 105.1 (s), 55.4 (s).

Bis(2-iodo-3-methoxyphenyl)ether **5**.[34] 1.00 g (4.34 mmol, 1.00 eq.) of bis(3-methoxyphenyl)ether were dissolved in 10 mL of dry THF and cooled in an ice/water bath. 6.16 mL (9.86 mmol, 2.27 eq.) of a 1.6 M *n*-hexane solution of *n*-butyllithium was slowly added. After the mixture was stirred at r.t. for 1 h it was cooled with an ice/water bath. To the yellow solution 2.69 g (9.55 mmol, 2.2 eq.) of 1,2-diiodoethane were slowly added and the solution was stirred at r t. overnight. The mixture was poured into 40 mL of a 10% aqueous solution of sodium bisulfite and the mixture was extracted with CH_2Cl_2 (3 x50 mL). The organic layer was washed with H_2O (70 mL) and brine (70 mL). The organic layer was dried over Na_2SO_4 and the solvent was evaporated in vacuum. The resulting crystals were washed with EtOH and cold *n*-hexane to afford a pale yellow solid (yield: 1.45 g, 69%). ^{1}H NMR (400 MHz, $CDCl_3$): δ [ppm] = 7.22 (t, $^3J_{H\text{-}H}$ = 8.2 Hz, 2H), 6.62 (dd, $^3J_{H\text{-}H}$ = 8.2 Hz, $^4J_{H\text{-}H}$ = 1.0 Hz, 2H), 6.42 (dd, $^3J_{H\text{-}H}$ = 8.2 Hz, $^4J_{H\text{-}H}$ = 1.0 Hz, 2H), 3.93 (s, 3H). ^{13}C NMR (151 MHz,

CD_2Cl_2): δ [ppm] = 160.2 (s), 157.5 (s), 130.0 (s), 111.6 (s), 106.3 (s), 81.0 (s). 56.8 (s).

10-(2′,6′-Difluorophenyl)-1,9-dimethoxy-10H-phenoxazine.[34] 2.00 g (4,15 mmol, 1.01 eq.) of compound **5**, 0.53 g (4.11 mmol 1.00 eq.) of 2,6-difluoroaniline, 1.19 g (12.40 mmol, 1.00 eq.) of NaO^{t}Bu, 0.21 g (0.21 mmol, 0.05 eq.) of $[Pd(dba)_3]\cdot CHCl_3$ and 1.8 mL (0.622 mmol, 0.15 eq.) of a 10% *n*-hexane solution of P^{t}Bu$_3$ were dissolved in 10 mL of dry toluene and heated under reflux for 16 h. After cooling to room temperature, the mixture was filtered through a pad of Celite and concentrated under vacuum until the solid product precipitated. The supernatant was filtered off and the remaining solid was washed with *n*-pentane (yield: 1.11 g, 75%). ^{1}H NMR (400 MHz, $CDCl_3$): δ [ppm] = 7.15 (tt, $^3J_{H\text{-}H}$ = 8.3 Hz, $^4J_{H\text{-}F}$ = 6.0 Hz, 1H), 6.94-6.82 (m, 4H), 6.56 (dd, $^3J_{H\text{-}H}$ = 8.2 Hz, $^4J_{H\text{-}H}$ = 1.1 Hz, 2H), 6.43 (dd, $^3J_{H\text{-}H}$ = 8.2 Hz, $J_{H\text{-}H}$ = 1.1 Hz, 2H), 3.64 (s, 6H).

10-(2′,6′-Difluorophenyl)-1,9-hydroxy-10H-phenoxazine.[34] 1.081 g (3.042 mmol, 1.0 eq.) of 10-(2′,6′-difluorophenyl)-1,9-dimethoxy-10*H*-phenoxazine were dissolved in 80 mL of dry DCM and cooled to −78 °C. 1.53 mL (4.035 g, 16.123 mmol, 5.3 eq.) of BBr_3 were slowly added whereupon the solution turned violet. After stirring at r.t. overnight the mixture was poured into 100 mL water and extracted with CH_2Cl_2 (3×50 mL). The organic phase was washed with H_2O (50 mL) and brine (2×50 mL), dried over Na_2SO_4 and the solvent was evaporated. The crude product was used without further purification.

2,2′:6′,2″:6″,6-Trioxytriphenylamine **6** (**TOTA**).[34] The crude 10-(2′,6′-difluorophenyl)-1,9-hydroxy-10*H*-phenoxazine and 2.144 g of K_2CO_3 (15.514 mmol, 5.1 eq.) were dissolved in 50 mL of dry DMF and stirred at 100 °C for 17 h. The mixture was poured into 100 mL of H_2O and a yellow solid precipitated. The precipitate was filtered off and washed with 150 mL of H_2O and 15 mL of *n*-pentane (yield: 0.77 g, 88%). ^{1}H NMR (400 MHz, C_6D_6): δ [ppm] = 6.30–6.23 (m, 9H). ^{13}C NMR (151 MHz, CD_2Cl_2): δ [ppm] = 142.7 (s), 123.7 (s), 117.3 (s), 111.5 (s).

4-Formyl-2,2′:6′,2″:6″,6-trioxytriphenylamine (***TOTA-CHO***).[38] 0.300 g (1.044 mmol, 1.0 eq.) of **TOTA** were dissolved in 21 mL of dry 1,4-dioxane and 8.04 mL (7.649 g, 104.504 mmol, 100.1 eq.) of dry DMF. $POCl_3$ (9.75 mL, 16.376 g, 106.801 mmol, 102 eq.) was added. The mixture was stirred under reflux conditions for 2 h. After cooling to r.t., the solution was poured into 100 mL of a 10% aqueous NaOH solution and extracted with CH_2Cl_2 (3×80 mL). The combined organic phases were washed with 100 mL of brine, dried over Na_2SO_4 and the solvent was evaporated under reduced pressure. The residue was subjected to silica gel column chromatography using toluene as the eluent to afford the product as an orange solid (yield: 0.18 g, 55%). ^{1}H NMR (400 MHz, $CDCl_3$): δ [ppm] = 9.35 (s, 1H, C*H*O), 6.75 (s, 2H, *H*1), 6.38–6.20 (m, 6H, *H*2-4). ^{13}C NMR (151 MHz, CD_2Cl_2): δ [ppm] = 189.3 (s), 142.2 (s), 142.1 (s), 124.8 (s), 114.9 (s), 113.1 (s), 112.0 (s), 111.6 (s), 29.9 (s).

TOTA-PTMH. A solution of 0.202 g (0.231 mmol, 1.0 eq.) of **PTM-PO(OEt)$_2$**. in 35 mL of dry THF was cooled to -78 °C and 0.064 g (0.554 mmol, 2.4 eq.) KO^{t}Bu were added. The resulting mixture was stirred for 20 min. and then allowed to warm to 0 °C. Then, 0.080 g (0.254 mmol, 1.1 eq.) of **TOTA-CHO** in 120 mL of dry THF were added. The solution was allowed to slowly warm to r.t. and stirred for 2 d. 90 mL of 2 N HCl were added, the phases were separated, and the aqueous phase was extracted with $CHCl_3$ (3×100 mL). The combined organic phases were washed with H_2O (1×100 mL), dried over Na_2SO_4 and the solvent was removed under reduced pressure. Purification was performed by silica gel column chromatography (*n*-pentane/EtOAc 10:1) to yield 50 mg (21%) of the product. ^{1}H NMR (600 MHz, CD_2Cl_2): δ [ppm] = 7.01 (s, 1H, *H*1), 6.87 (d, $^3J_{H\text{-}H}$ = 16.5 Hz, 1H, *H*3), 6.83 (d, $^3J_{H\text{-}H}$ = 16.5 Hz, 1H, *H*2), 6.70 (t, $^3J_{H\text{-}H}$ = 8.3 Hz, 2H, *H*11), 6.64 (s, 2H, *H*5), 6.48-6.44 (m, 4H, *H*10, *H*12). ^{13}C NMR (151 MHz, CD_2Cl_2): δ [ppm] = 142.5 (s, *C*8), 142.5 (s, *C*7), 142.3 (s, *C*13), 137.2 (s), 137.2 (s, *C*3), 136.7 (s), 136.7 (s), 136.1 (s), 135.3 (s), 135.2 (s), 135.0 (s), 134.1 (s), 134.1 (s), 134.1 (s), 133.8 (s), 133.8 (s), 133.7 (s), 133.6 (s), 133.4 (s), 132.6 (s), 132.6 (s), 132.3 (s), 132.0 (s, *C*4), 124.1 (s, *C*11), 122.3 (s, *C*2), 117.4 (s, *C*6), 116.32 (s, *C*9), 111.7 (s, *C*10/*C*12), 111.6 (s, *C*10/*C*12), 110.1 (s, *C*5), 56.75 (s, *C*1). FTIR: 2921 (w), 2851 (w), 1593 (w), 1504 (m), 1321 (w), 1259 (m), 1178 (w), 1159 (w), 1063 (w), 1033 (w), 946 (w), 861 (w), 809 (w), 759 (w), 704 (w), 676 (w). MALDI HRMS (DCTB, positive mode) calcd. for $C_{39}H_{11}Cl_{14}NO_3$ 1036.6290 $[M]^+$, found 1036.6282. Anal. Calcd. for $C_{39}H_{11}Cl_{14}NO_3$: C, 45.14; H, 1.07; N, 1.35; Found: C, 45.38; H, 1.91; N, 1.36.

TOTA-PTM•. To a suspension of 100 mg (0.092 mmol, 1 eq.) **TOTA-PTMH** in 20 mL of dry DMSO 21 mg (0.185 mmol, 2 eq.) of KO^{t}Bu were added. The purple solution was stirred in the dark for 1.5 h and then 23 mg (0.092, 1 eq.) of chloranil were added. After further stirring for 1.5 h in the dark the solvent was evaporated. Purification followed by silica gel column chromatography using DCM as eluent and the crude product was precipitated twice by dissolving it in DCM and adding it dropwise to methanol (yield: 53 mg, 53%). FTIR: 2981 (w), 2932 (w), 1593 (w), 1502 (m), 1322 (w), 1259 (m), 1178 (w), 1259 (w), 1063 (w), 946 (w), 809 (m), 705 (w). MALDI HRMS (DCTB, positive mode) calcd. for $C_{39}H_{10}Cl_{14}NO_3$ 1035.6212 $[M]^+$, found 1035.6210. Anal. Calcd. for $C_{39}H_{10}Cl_{14}NO_3$: C, 45.18; H, 0.97; N, 1.35; Found: C, 45.78; H, 1.68; N, 1.40.

1-[Bis(2,3,4,5,6-pentachlorophenyl)methyl]-4-[2-(4-iodophenyl)ethenyl]-2,3,5,6-tetrachlorobenzene **8**.[35] To a suspension of 2.000 g (1.849 mmol, 1.00 eq.) of **PTM-PPh$_3$Br** in 55 mL of dry THF 0.207 g (1.849 mmol, 1.00 eq.) of KO^{t}Bu were added. After stirring for 1 h at r.t. 0.349 g (1.885 mmol, 1.02 eq.) of 4-iodobenzaldehyde **7** were added and stirring was continued overnight. The mixture was quenched with 15 mL of 1 M HCl and the suspension was stirred for 1 h. The phases were separated, and the aqueous phase was extracted with $CHCl_3$ (3×80 mL). The combined organic phase was washed with H_2O (3×80 mL), dried over Na_2SO_4 and the solvent was evaporated. Purification was achieved by silica gel column chromatography with *n*-hexane as the eluent (yield: 1.103 g, 62%). ^{1}H NMR (400 MHz, $CDCl_3$): δ [ppm] = 7.74 (d, $^3J_{H\text{-}H}$ = 8.3 Hz, 2H, *H*5), 7.27 (d, $^3J_{H\text{-}H}$ = 8.3 Hz, 2H, *H*4), 7.06 (d, $^3J_{H\text{-}H}$ = 16.6 Hz, 1H, *H*2), 7.02 (s, 1H, *H*1), 6.99 (d, $^3J_{H\text{-}H}$ = 16.6 Hz, 1H, *H*3). ^{13}C NMR (151 MHz, CD_2Cl_2): δ [ppm] = 138.1 (s), 137.8 (s), 137.5 (s), 137.3 (s), 136.7 (s), 136.6 (s), 136.4 (s), 135.6 (s), 135.2 (s), 135.2 (s), 135.0 (s), 134.1 (s), 133.8 (s), 133.9 (s), 133.7 (s), 133.7 (s), 133.5 (s), 133.4 (s), 132.6 (s), 132.4 (s), 129.8 (s), 128.7 (s), 125.2 (s), 123.9 (s), 94.7 (s), 94.3 (s), 56.8 (s).

TPAN-PTMH. 0.790 g (0.828 mmol, 1.00 eq.) of compound **8** and 0.232 g (0.910 mmol, 1.10 eq.) of bis(dimethylaminophenyl)amine were dissolved in 30 mL of dry toluene and 0.043 g (0.041 mmol, 0.05 eq.) $[Pd_2(dba)_3]\cdot CHCl_3$, 0.1 mL (0.033 mmol, 0.04 eq.) of a 10% *n*-hexane solution of P^{t}Bu$_3$ and 0.199 g (2.069 mmol, 2.5 eq.) of K_2CO_3 were added. The mixture was heated under reflux for 22 h and the solvent was removed. The residue was dissolved in 100 mL of CH_2Cl_2, washed with H_2O (3×80 mL), dried over Na_2SO_4 and the solvent was removed. Column chromatography over silica gel (*n*-pentane/EtOAc/NEt$_3$ 10:1:0.1) yielded 0.295 g, 33%) of the product. ^{1}H NMR (600 MHz, CD_2Cl_2): δ [ppm] = 7.31 (d, $^3J_{H\text{-}H}$ = 8.8 Hz, 2H, *H*5), 7.08-6.95 (m, 6H, *H*1, *H*3, *H*9), 6.87 (d, $^3J_{H\text{-}H}$ = 16.5 Hz, 1H, *H*2), 6.82 (d, $^3J_{H\text{-}H}$ = 8.8 Hz, 2H, *H*6), 6.70 (d, $^3J_{H\text{-}H}$ = 8.9 Hz, 4H, *H*10), 2.93 (s, 12H, N(C*H*$_3$)$_2$). ^{13}C NMR (151 MHz, CD_2Cl_2): δ [ppm] = 150.7 (s, *C*7), 148.4 (s, *C*11), 138.8 (s, *C*3) 138.6 (s), 137.2 (s), 137.2 (s), 136.9 (s, *C*8), 135.6 (s), 135.5 (s), 135.4 (s), 135.0 (s), 134.5 (s), 134.4 (s), 134.2 (s), 133.9 (s), 133.9 (s), 133.8 (s), 133.8 (s), 133.6 (s), 132.8 (s), 132.8 (s), 132.5 (s), 128.0 (s, *C*5), 127.6 (s, *C*9), 126.5(s, *C*4), 119.3 (s, *C*2), 118.3 (s, *C*6), 113.8 (s, *C*10), 57.0 (s, *C*1), 41.0 (s, *C*12). FT-IR: 3661 (w), 2980 (m), 2890 (w), 1595 (w), 1505 (m), 1381 (w), 1323 (w), 1290 (w), 1259 (w), 1159 (m), 1071 (w), 948 (w), 808 (m), 704 (w).

MALDI HRMS (DCTB, positive mode) calcd. for $C_{43}H_{27}Cl_{14}N_3$ 1080.7756 $[M]^+$, found: 1080.7750. Anal. Calcd. for $C_{43}H_{27}Cl_{14}N_3 \cdot C_7H_8$ (as detected by NMR): C, 51.15; H, 3.00; N, 3.58; Found: C, 51.52; H, 3.35; N, 3.85.

TPAN-PTM•. To a suspension of 100 mg (0.092 mmol, 1 eq.) of **TPAN-PTMH** in 20 mL of dry DMSO, 21 mg (0.185 mmol, 2 eq.) of KO^{t}Bu were added and stirred at room temperature for 1.5 h in the dark. 23 mg (0.092 mmol, 1 eq.) of tetrachloro-1,4-benzoquinone were added and the solution was stirred for 1.5 h and the solvent was evaporated. The residue was subjected to silica gel column chromatography using DCM as eluent. Further purification was achieved by adding a concentrated CH_2Cl_2 solution of the crude product dropwise to methanol (2 times) to yield 58 mg, 53% of the target compound. FT-IR: 2923 (w), 2852 (w), 1592 (w), 1502 (m), 1442 (w), 1322 (w), 1259 (w), 1227 (w), 1178 (w), 1159 (w), 1061 (w), 946 (w), 811 (w), 768 (w), 713 (w). MALDI HRMS (DCTB, positive mode) calcd. for $C_{43}H_{26}Cl_{14}N_3$ 1079.7678 $[M]^+$, found: 1079.7672. Anal. Calcd. for $C_{43}H_{27}Cl_{14}N_3 \cdot C_7H_8$: C, 51.19; H, 2.92; N, 3.58; Found: C, 51.83; H, 3.94; N, 3.53.

Acknowledgements

We gratefully acknowledge financial support of this work by the Deutsche Forschungsgemeinschaft (DFG, German Research Foundation) – SFB 767 – Project-ID 32152442 (project C14) and grant number INST 40/467-1 FUGG (JUSTUS cluster). We also wish to thank the reviewers for their insightful comments and suggestions. Open access funding enabled and organized by Projekt DEAL.

Conflict of Interest

The authors declare no conflict of interest.

Keywords: Donor-acceptor dyads · EPR spectroscopy · PTM radical · Spectroelectrochemistry · TOTA

[1] O. Kahn, J. P. Launay, *Chemtronics* **1988**, *3*, 140.
[2] C. Roux, D. M. Adams, J. P. Itié, A. Polian, D. N. Hendrickson, M. Verdaguer, *Inorg. Chem.* **1996**, *35*, 2846.
[3] a) A. Caneschi, A. Cornia, A. Dei, *Inorg. Chem.* **1998**, *37*, 3419; b) D. Ruiz, J. Yoo, D. N. Hendrickson, I. A. Guzei, A. L. Rheingold, *Chem. Commun.* **1998**, 2089; c) D. Ruiz-Molina, J. Veciana, K. Wurst, D. N. Hendrickson, C. Rovira, *Inorg. Chem.* **2000**, *39*, 617; d) G. Speier, Z. Tyeklár, P. Tóth, E. Speier, S. Tisza, A. Rockenbauer, A. M. Whalen, N. Alkire, C. G. Pierpont, *Inorg. Chem.* **2001**, *40*, 5653; e) S. H. Bodnar, A. Caneschi, A. Dei, D. A. Shultz, L. Sorace, *Chem. Commun.* **2001**, 2150; f) W. Kaim, B. Schwederski, *Coord. Chem. Rev.* **2010**, *254*, 1580; g) D. Schweinfurth, F. Weisser, B. Sarkar, *Nachr. Chem.* **2009**, *57*, 862; h) W. Kaim, *Eur. J. Inorg. Chem.* **2012**, *2012*, 343; i) W. Kaim, *Inorg. Chem.* **2011**, *50*, 9752; j) A. Dei, L. Sorace, *Appl. Magn. Reson.* **2010**, *38*, 139; k) M. Mitsumi, Y. Komatsu, M. Hashimoto, K. Toriumi, Y. Kitagawa, Y. Miyazaki, H. Akutsu, H. Akashi, *Chem. Eur. J.* **2021**, *27*, 3074.
[4] C. G. Pierpont, *Coord. Chem. Rev.* **2001**, *216–217*, 99.
[5] a) T. Ito, N. Imai, T. Yamaguchi, T. Hamaguchi, C. H. Londergan, C. P. Kubiak, *Angew. Chem. Int. Ed.* **2004**, *43*, 1376; b) M. Lohan, F. Justaud, T. Roisnel, P. Ecorchard, H. Lang, C. Lapinte, *Organometallics* **2010**, *29*, 4804; c) M. Lohan, F. Justaud, H. Lang, C. Lapinte, *Organometallics* **2012**, *31*, 3565; d) R. Sakamoto, K. P. Rao, H. Nishihara, *Chem. Lett.* **2011**, *40*, 1316; e) E. C. Fitzgerald, A. Ladjarafi, N. J. Brown, D. Collison, K. Costuas, R. Edge, J.-F. Halet, F. Justaud, P. J. Low, H. Meghezzi, T. Roisnel, M. W. Whiteley, C. Lapinte, *Organometallics* **2011**, *30*, 4180; f) J. Chen, E. Wuttke, W. Polit, T. Exner, R. F. Winter, *J. Am. Chem. Soc.* **2013**, *135*, 3391; g) C. Hassenrück, P. Mücke, J. Scheck, S. Demeshko, R. F. Winter, *Eur. J. Inorg. Chem.* **2017**, *2017*, 401; h) C. Hassenrück, M. Azarkh, M. Drescher, M. Linseis, S. Demeshko, F. Meyer, R. F. Winter, *Organometallics* **2020**, *39*, 153; i) G. K. Lahiri, A. Singh, S. Panda, S. Dey, *Angew. Chem. Int. Ed. Engl.* **2021**; j) K. P. Rao, T. Kusamoto, F. Toshimitsu, K. Inayoshi, S. Kume, R. Sakamoto, H. Nishihara, *J. Am. Chem. Soc.* **2010**, *132*, 12472; k) A. Neidlinger, C. Förster, K. Heinze, *Eur. J. Org. Chem.* **2016**, *2016*, 4852.
[6] T. Tezgerevska, K. G. Alley, C. Boskovic, *Coord. Chem. Rev.* **2014**, *268*, 23.
[7] a) T. Bally, *Nat. Chem.* **2010**, *2*, 165; b) B. Müller, T. Bally, F. Gerson, A. de Meijere, M. von Seebach, *J. Am. Chem. Soc.* **2003**, *125*, 13776; c) F. F. Puschmann, J. Harmer, D. Stein, H. Rüegger, B. de Bruin, H. Grützmacher, *Angew. Chem. Int. Ed. Engl.* **2010**, *49*, 385.
[8] a) J. S. Miller, M. Drillon, *Shultz, D. A. In:. Magnetoscience-From Molecules to Materials*, Wiley-VCH, New York, **2000**; b) P. Gütlich, A. Dei, *Angew. Chem. Int. Ed.* **1997**, *36*, 2734.
[9] a) O. Sato, J. Tao, Y.-Z. Zhang, *Angew. Chem. Int. Ed.* **2007**, *46*, 2152; b) O. Sato, S. Hayami, Z.-z. Gu, K. Takahashi, R. Nakajima, A. Fujishima, *Chem. Phys. Lett.* **2002**, *355*, 169; c) H. W. Liu, K. Matsuda, Z. Z. Gu, K. Takahashi, A. L. Cui, R. Nakajima, A. Fujishima, O. Sato, *Phys. Rev. Lett.* **2003**, *90*, 167403; d) A. Hauser, J. Jeftić, H. Romstedt, R. Hinek, H. Spiering, *Coord. Chem. Rev.* **1999**, *190–192*, 471; e) P. Gütlich, *Coord. Chem. Rev.* **2001**, *219–221*, 839; f) A. Ghosh, T. Wondimagegn, E. Gonzalez, I. Halvorsen, *J. Inorg. Biochem.* **2000**, *78*, 79; g) A. Dei, *Angew. Chem. Int. Ed.* **2005**, *44*, 1160; h) N. A. Vázquez-Mera, F. Novio, C. Roscini, C. Bellacanzone, M. Guardingo, J. Hernando, D. Ruiz-Molina, *J. Mater. Chem. C* **2016**, *4*, 5879.
[10] I. Ratera, C. Sporer, D. Ruiz-Molina, N. Ventosa, J. Baggerman, A. M. Brouwer, C. Rovira, J. Veciana, *J. Am. Chem. Soc.* **2007**, *129*, 6117.
[11] I. Ratera, D. Ruiz-Molina, F. Renz, J. Ensling, K. Wurst, C. Rovira, P. Gütlich, J. Veciana, *J. Am. Chem. Soc.* **2003**, *125*, 1462.
[12] a) O. Elsner, D. Ruiz-Molina, I. Ratera, J. Vidal-Gancedo, C. Rovira, J. Veciana, *J. Organomet. Chem.* **2001**, *637–639*, 251; b) O. Elsner, D. Ruiz-Molina, J. Vidal-Gancedo, C. Rovira, J. Veciana, *Chem. Commun.* **1999**, 579.
[13] G. D'Avino, L. Grisanti, J. Guasch, I. Ratera, J. Veciana, A. Painelli, *J. Am. Chem. Soc.* **2008**, *130*, 12064.
[14] a) M. Ballester, J. Riera, J. Castañer, C. Badía, J. M. Monsó, *J. Am. Chem. Soc.* **1971**, *93*, 2215; b) V. Lloveras, J. Vidal-Gancedo, D. Ruiz-Molina, T. M. Figueira-Duarte, J.-F. Nierengarten, J. Veciana, C. Rovira, *Faraday Discuss.* **2006**, *131*, 291–305; discussion 307–24; c) C. Sporer, I. Ratera, D. Ruiz-Molina, J. Vidal Gancedo, K. Wurst, P. Jaitner, C. Rovira, J. Veciana, *J. Phys. Chem. Solids* **2004**, *65*, 753; d) C. Sporer, I. Ratera, D. Ruiz-Molina, Y. Zhao, J. Vidal-Gancedo, K. Wurst, P. Jaitner, K. Clays, A. Persoons, C. Rovira, J. Veciana *Angew. Chem. Int. Ed.* **2004**, *43*, 5266.
[15] G. D'Avino, L. Grisanti, A. Painelli, J. Guasch, I. Ratera, J. Veciana, *CrystEngComm* **2009**, *11*, 2040.
[16] J. Guasch, L. Grisanti, S. Jung, D. Morales, G. D'Avino, M. Souto, X. Fontrodona, A. Painelli, F. Renz, I. Ratera, J. Veciana, *Chem. Mater.* **2013**, *25*, 808.
[17] a) J. Guasch, N. Crivillers, M. Souto, I. Ratera, C. Rovira, P. Samorì, J. Veciana, *J. Appl. Phys.* **2019**, *125*, 142909; b) S. Nishida, Y. Morita, K. Fukui, K. Sato, D. Shiomi, T. Takui, K. Nakasuji, *Angew. Chem. Int. Ed.* **2005**, *44*, 7277.
[18] J. Guasch, L. Grisanti, V. Lloveras, J. Vidal-Gancedo, M. Souto, D. C. Morales, M. Vilaseca, C. Sissa, A. Painelli, I. Ratera, C. Rovira, J. Veciana, *Angew. Chem. Int. Ed.* **2012**, *51*, 11024.
[19] M. Souto, D. C. Morales, J. Guasch, I. Ratera, C. Rovira, A. Painelli, J. Veciana, *J. Phys. Org. Chem.* **2014**, *27*, 465.
[20] A. Heckmann, C. Lambert, M. Goebel, R. Wortmann, *Angew. Chem. Int. Ed.* **2004**, *43*, 5851.
[21] S. Dümmler, W. Roth, I. Fischer, A. Heckmann, C. Lambert, *Chem. Phys. Lett.* **2005**, *408*, 264.
[22] A. Heckmann, C. Lambert, *J. Am. Chem. Soc.* **2007**, *129*, 5515.
[23] D. Reitzenstein, T. Quast, F. Kanal, M. Kullmann, S. Ruetzel, M. S. Hammer, C. Deibel, V. Dyakonov, T. Brixner, C. Lambert, *Chem. Mater.* **2010**, *22*, 6641.
[24] a) S. F. Nelsen, R. F. Ismagilov, *J. Phys. Chem. A* **1999**, *103*, 5373; b) R. L. Blackbourn, J. T. Hupp, *J. Phys. Chem.* **1990**, *94*, 1788.
[25] V. Gamero, D. Velasco, S. Latorre, F. López-Calahorra, E. Brillas, L. Juliá, *Tetrahedron Lett.* **2006**, *47*, 2305.
[26] D. Velasco, S. Castellanos, M. López, F. López-Calahorra, E. Brillas, L. Julia, *J. Org. Chem.* **2007**, *72*, 7523.
[27] S. Castellanos, D. Velasco, F. López-Calahorra, E. Brillas, L. Julia, *J. Org. Chem.* **2008**, *73*, 3759.

[28] L. Fajarí, R. Papoular, M. Reig, E. Brillas, J. L. Jorda, O. Vallcorba, J. Rius, D. Velasco, L. Juliá, *J. Org. Chem.* **2014**, *79*, 1771.
[29] A. Gilabert, L. Fajarí, I. Sirés, M. Reig, E. Brillas, D. Velasco, J. M. Anglada, L. Juliá, *New J. Chem.* **2017**, *41*, 8422.
[30] P. Ballesteros, A. Cuadrado, A. Gilabert, L. Fajarí, I. Sirés, E. Brillas, M. P. Almajano, D. Velasco, J. M. Anglada, L. Juliá, *Phys. Chem. Chem. Phys.* **2019**, *21*, 20225.
[31] R. F. Winter, L. A. Casper, M. Linseis, S. Demeshko, M. Azarkh, M. Drescher, *Chem. Eur. J.* **2021**, doi.org/10.1002/chem.202101032.
[32] M. Kuratsu, M. Kozaki, K. Okada, *Angew. Chem. Int. Ed.* **2005**, *44*, 4056.
[33] M. Kuratsu, S. Suzuki, M. Kozaki, D. Shiomi, K. Sato, T. Takui, K. Okada, *Inorg. Chem.* **2007**, *46*, 10153.
[34] S. Suzuki, N. Tanaka, M. Kozaki, D. Shiomi, K. Sato, T. Takui, K. Okada, *Chem. Eur. J.* **2017**, *23*, 16014.
[35] C. Rovira, D. Ruiz-Molina, O. Elsner, J. Vidal-Gancedo, J. Bonvoisin, J.-P. Launay, J. Veciana, *Chem. Eur. J.* **2001**, *7*, 240.
[36] M. Ballester, J. Castañer, J. Riera, A. Ibanez, J. Pujadas, *J. Org. Chem.* **1982**, *47*, 259.
[37] F. Yang, J. Zhao, Y. Li, S. Zhang, Y. Shao, H. Shao, T. Ma, C. Gong, *Eur. Polym. J.* **2009**, *45*, 2053.
[38] M. Kuratsu, S. Suzuki, M. Kozaki, D. Shiomi, K. Sato, T. Takui, T. Kanzawa, Y. Hosokoshi, X.-Z. Lan, Y. Miyazaki, A. Inaba, K. Okada, *Chem. Asian J.* **2012**, *7*, 1604.
[39] V. Dvořák, I. Němec, J. Zýka, *Microchem. J.* **1967**, *12*, 350.
[40] V. Lloveras, J. Vidal-Gancedo, T. M. Figueira-Duarte, J.-F. Nierengarten, J. J. Novoa, F. Mota, N. Ventosa, C. Rovira, J. Veciana, *J. Am. Chem. Soc.* **2011**, *133*, 5818.
[41] F. Pragst, R. Ziebig, E. Boche, *J. Lumin.* **1979**, *21*, 21.
[42] M. Souto, J. Calbo, I. Ratera, E. Ortí, J. Veciana, *Chem. Eur. J.* **2017**, *23*, 11067.
[43] a) M. Ballester, J. Riera-Figueras, J. Castaner, C. Badfa, J. M. Monso, *J. Am. Chem. Soc.* **1971**, *93*, 2215; b) M. Ballester, J. Castaner, J. Riera, A. Ibanez, J. Pujadas, *J. Org. Chem.* **1982**, *47*, 259.
[44] M. Souto, M. V. Solano, M. Jensen, D. Bendixen, F. Delchiaro, A. Girlando, A. Painelli, J. O. Jeppesen, C. Rovira, I. Ratera, J. Veciana, *Chem. Eur. J.* **2015**, *21*, 8816.
[45] L. Grisanti, G. D'Avino, A. Painelli, J. Guasch, I. Ratera, J. Veciana, *J. Phys. Chem. B* **2009**, *113*, 4718.
[46] M. Krejčik, M. Daněk, F. Hartl, *J. Electroanal. Chem.* **1991**, *317*, 179.
[47] a) S. Amthor, B. Noller, C. Lambert, *Chem. Phys.* **2005**, *316*, 141; b) S. Dapperheld, E. Steckhan, K.-H. G. Brinkhaus, T. Esch, *Chem. Ber.* **1991**, *124*, 2557; c) C. Quinton, V. Alain-Rizzo, C. Dumas-Verdes, F. Miomandre, G. Clavier, P. Audebert, *RSC Adv.* **2014**, *4*, 34332.
[48] a) M. Dibrelle, R. Hoekstra, M. N. Weaver, K. Okada, S. F. Nelsen, J. I. Zink, *J. Phys. Org. Chem.* **2012**, *25*, 578; b) Y. Nakano, H. Yamochi, G. Saito, M. Kuratsu, K. Okada, *J. Phys. Conf. Ser.* **2008**, *132*, 12024.
[49] A. Bobet, A. Cuadrado, L. Fajarí, I. Sirés, E. Brillas, M. P. Almajano, V. Jankauskas, D. Velasco, L. Juliá, *J. Phys. Org. Chem.* **2019**, *32*, e3974.
[50] M. Abe, *Chem. Rev.* **2013**, *113*, 7011.
[51] S. Stoll, A. Schweiger, *J. Magn. Reson.* **2006**, *178*, 42.
[52] O. Chen, J. Zhuang, F. Guzzetta, J. Lynch, A. Angerhofer, Y. C. Cao, *J. Am. Chem. Soc.* **2009**, *131*, 12542.
[53] M. J. Frisch, G. Trucks, H. B. Schlegel, G. E. Scuseria, M. A. Robb, J. R. Cheesman, G. Scalmani, V. Barone, B. Mennucci, G. A. Petersson, H. Nakatsuji, M. Caricato, X. Li, H. P. Hratchian, A. F. Izmaylov, J. Blonio, G. Zheng, J. L. Sonnenberg, M. Hada, M. Ehara, K. Toyota, R. Fukuda, J. Hasegawa, M. Ishida, T. Nakajima, Y. Honda, O. Kitao, H. Nakai, T. Vreven, J. A. Montgomery Jr., J. E. Peralta, F. Ogliaro, M. Bearpark, J. J. Heyd, E. Brothers,K. N. Kudin, V. N. Staroverov, T. Keith, R. Kobayashi, J. Normand, K. Raghavachari, A. Rendell, J. C. Burant, S. S. Iyengar,J. Tomasi, M. Cossi, N. Rega, J. M. Millam, M. Klene, J. E. Knox,J. B. Cross, V. Bakken, C. Adamo, J. Jaramillo, R. Gomperts, R. E. Stratmann, O. Yazyev, A. J. Austin, R. Cammi, C. Pomelli, J. W. Ochterski, R. L. Martin, K. Morokuma, V. G. Zakrzewski, G. A. Voth, P. Salvador, J. Dannenberg, S. Dapprich, A. D. Daniels, Ö. Farkas, J. B. Foresman, J. V. Ortiz, J. Cioslowski, D. J. Fox, *Gaussian 09, revision B.01, Gaussian Inc.: Wallingford, CT* **2010**.
[54] M. Cossi, N. Rega, G. Scalmani, V. Barone, *J. Comput. Chem.* **2003**, *24*, 669.
[55] J. P. Perdew, K. Burke, M. Ernzerhof, *Phys. Rev. Lett.* **1996**, *77*, 3865.
[56] N. M. O'Boyle, A. L. Tenderholt, K. M. Langner, *J. Comput. Chem.* **2008**, *29*, 839.
[57] M. D. Hanwell, D. E. Curtis, D. C. Lonie, T. Vandermeersch, E. Zurek, Hutchison, G. R. Avogadro, *J. Cheminf.* **2012**, *4*, 1.
[58] O. Tange, *USENIX Magazine* **2011**, *36*, 42.
[59] J.-L. Muñoz-Gómez, I. Marín-Montesinos, V. Lloveras, M. Pons, J. Vidal-Gancedo, J. Veciana, *Org. Lett.* **2014**, *16*, 5402.
[60] M. Ballester, J. Veciana, J. Riera, J. Castaner, C. Rovira, O. Armet, *J. Org. Chem.* **1986**, *51*, 2472.

Manuscript received: April 17, 2021
Revised manuscript received: July 19, 2021
Accepted manuscript online: July 26, 2021